

Optoionic Sensing

Baohong Chen and Zhigang Suo*

The eye converts an optical signal to an ionic signal. This transduction is mimicked here using a photodiode in contact with ionic conductors, such as hydrogels. Photons generate electron-hole pairs in the photodiode. The photodiode/hydrogel interface forms capacitive coupling so that movements of electrons and holes in the photodiode induce movements of ions in the hydrogels. The hydrogels can be readily made stretchable and biocompatible to mimic the function of nerves. When light is turned on and off, the voltage between the hydrogels responds within 10 ms, comparable to the response in the human eye. A photosensitive skin is demonstrated to generate a voltage in response to light but not to stretch. Furthermore, a photosensitive actuation is demonstrated to mimic the light-triggered reflex, such as blinking of the eye and camouflage of the skin. Optoionic transduction has potential applications for wearable devices, implantable devices, and robotics.

1. Introduction

In animals and plants, light-gated ion channels convert optical signals to electrical signals (Figure 1a).^[1] The anatomy and physiology of such a living system have been mimicked in the development of artificial optoelectrical transduction. Examples include laser-tuned ion channels^[2] and droplet bilayers.^[3] But the anatomical and physiological mimics are difficult to integrate, control, and maintain. An alternative approach is to mimic the function, not the anatomy and physiology. For example, a semiconductor photodiode converts an optical signal to an electronic signal. However, the semiconductor mechanically mismatches with living tissues. By contrast, ionic conductors, such as hydrogels, can be readily made stretchable and biocompatible.^[4] A visual-haptic fusion has been demonstrated recently using photodiodes, pressure sensors, and hydrogel interconnects.^[5]

Optoionic transduction provides a component to mimic complex biological functions. In addition to the retina, many living systems, such as plants, bacteria, and some animals, sense light through photosensitive skins or exoskeletons.^[6] In animals, the sense of light generates neuromuscular responses.^[7] For example, humans tend to close their eyes in response to strong light. These more complex functions require components in

addition to optoionic transduction. For example, hydrogels have been used to enable actuators,^[8] artificial axons,^[9] and tunable ionic eyes.^[10] The biocompatibility of hydrogels makes them suitable for bio-electronic interfaces.^[11,12] In an integrated system, artificial muscles control an ionic lens to focus the light onto an optoionic sensor, the sensor receives photons and generates ionic signals, and the ionic signals transmit via artificial axons to activate neurons (Figure S1, Supporting Information).

Here we study the physics of photodiode-hydrogel hybrids and explore their applications. An interface between a photodiode and a hydrogel functions as a capacitor, which can be charged by light.


To mimic the behavior of the eye, we present strategies that convert both cyclic and steady irradiations of light to cyclic ionic signals. The frequency of ionic signals achieves the frequency of neural signals (several hundred Hertz). We demonstrate a photosensitive skin that responds to lights but not to deformation. We achieve an artificial photosensitive neuromuscular response through the combination of optoionic transduction, transistor, and electrochemical reaction.

2. Characterizations of Photodiode-Hydrogel Hybrids

A photodiode-hydrogel hybrid enables optoionic transduction (Figure 1b). The photodiode consists of a semiconductor *p-n* junction, and the hydrogel contains mobile ions. When a beam of light shines upon the photodiode, pairs of electrons and holes are generated, which drift in the opposite directions, driven by the built-in electric field of the *p-n* junction. The interface between the photodiode and the hydrogel is assumed to undergo no electrochemical reaction but acts like a capacitor. In response to the movements of the electrons and holes in the photodiode, ions of opposite signs move in the hydrogel. Consequently, the change of light charges or discharges the photodiode/hydrogel interface. This process converts an optical signal to an ionic signal. The ionic signal transmits through the ionic conductor to a terminal.

We characterize an optoionic sensor as follows. A photodiode is sandwiched between two ionic conductors, sealed in dielectrics, and connected through electronic conductors to an external circuit (Figure 1c). The optoionic sensor is placed in a homemade chamber consisting of a metal-plastic bilayer, which shields the interior from external light, electrostatic field, and electromagnetic field (Figure 1d). Inside the chamber, we install

B. Chen, Z. Suo
John A. Paulson School of Engineering and Applied Sciences
Kavli Institute for Bionano Science and Technology
Harvard University
Cambridge, MA 02138, USA
E-mail: suo@seas.harvard.edu

 The ORCID identification number(s) for the author(s) of this article can be found under <https://doi.org/10.1002/sml.202103882>.

DOI: 10.1002/sml.202103882

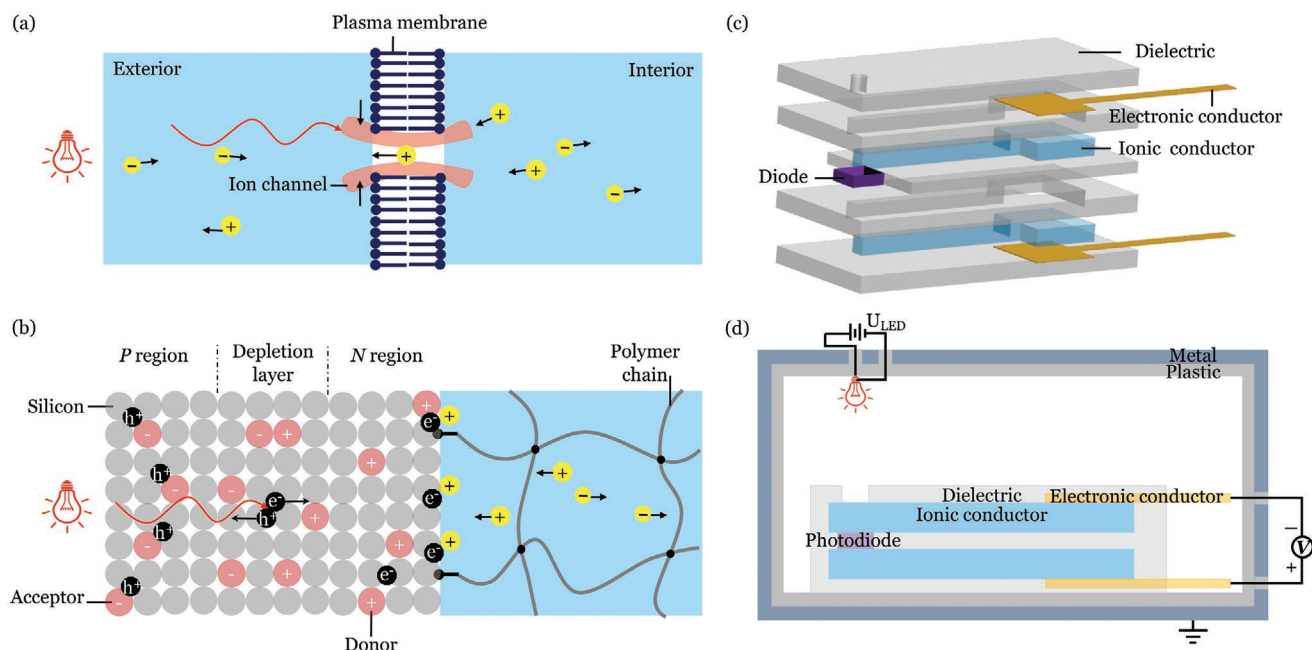


Figure 1. Optoionics inspired by the eye. a) In the eye, light triggers an ion channel to close, and the process converts an optical signal to an ionic signal. b) In mimicry, light generates electrons and holes in a photodiode, and the built-in electric field in the diode moves electrons and holes, causing the ions to move in a hydrogel. c) Assembly of a sample, where the photodiode is sandwiched by ionic conductors. d) The sample is put in an opaque chamber for the measurements.

a white light LED and control the intensity of light by applying a voltage U_{LED} . When the LED is turned on, the photodiode generates electron-hole pairs. By using a highly transparent ionic conductor, visible light can transmit to the photodiode. For instance, a 1 mm-thick polyacrylamide hydrogel has an average transmittance of visible light larger than 98%.^[13]

2.1. Response to Cyclic Irradiation of Light

We have studied several configurations connecting photodiodes, dielectrics, ionic conductors, and electronic conductors (Figure S2, Supporting Information). We will describe one configuration in the body of the paper (Figure 2a). We connect the sensor through the two hydrogels to a resistor R and measure the voltage U over the resistor. The two ionic conductors are separated by a layer of dielectric elastomer (Figure 1d). This sandwich design forms an ionic cable.^[9] The ionic cable mimics an axon so that the photodiode can be at some distance from the voltmeter. When the light is switched on and off at a low frequency (1 Hz), the peak voltage increases with the load resistance R (Figure 2b). The output power, U^2/R , reaches the maximum when the load resistance is $R = 5 \text{ k}\Omega$. To mimic an unmyelinated human optic nerve, which has a representative transmembrane resistance $\approx 10 \text{ M}\Omega$,^[14] we connect a resistor of $10 \text{ M}\Omega$ to the optoionic sensor. The output voltage and power decay with the frequency range 1 to 100 Hz (Figure 2c).

We remove the resistor R and measure the open-circuit voltage (Figure 2d). The light is switched on and off at a frequency of 1 Hz. The transition time of voltage response is

$\approx 1\text{--}10 \text{ ms}$ (Figure 2e,f). This response time is comparable to that in the human eye. We systematically measure the open-circuit voltages and on-and-off transition time of the other configurations as well (Figure S2, Supporting Information). We represent the sensor using an equivalent circuit (Figure S3e, Supporting Information), the estimated transition time is $\approx 1 \text{ ms}$, and the estimated decay time is $\approx 10 \text{ s}$.

2.2. Convert Steady Irradiation of Light into Cyclic Ionic Signal

When a steady light shines over a photodiode, the voltage becomes constant after some time. However, under a steady light, nerve signals in the eyes are cyclic.^[1] To mimic the cyclic nerve signal by ionic signals under the steady light irradiation, we control a bipolar transistor to discharge the photodiode (Figure 2g, supplementary context 1.5). The transistor acts as a switch under the control of a voltage U_{BE} applied by a function generator. The photodiode is short-circuited through C and E terminals when a voltage U_{BE} beyond the threshold (0.6 V) is applied between B and E terminals. The photodiode is open-circuited through C and E terminals when voltage U_{BE} is less than the threshold. The equivalent circuits of the two states are shown in Figure S7, Supporting Information. The amplitude of output voltage measured between ionic conductors corresponds to the intensity of steady light, but the frequency is the same as the switching frequency of the transistor (1 Hz, Figure 2h). A larger U_{BE} applied to the transistor will not change the amplitude of ionic signals (Figure 2i). We further show the frequency responses up to the frequency of nerve signals ($\approx 10^2 \text{ Hz}$) (Figure S9, Supporting Information).

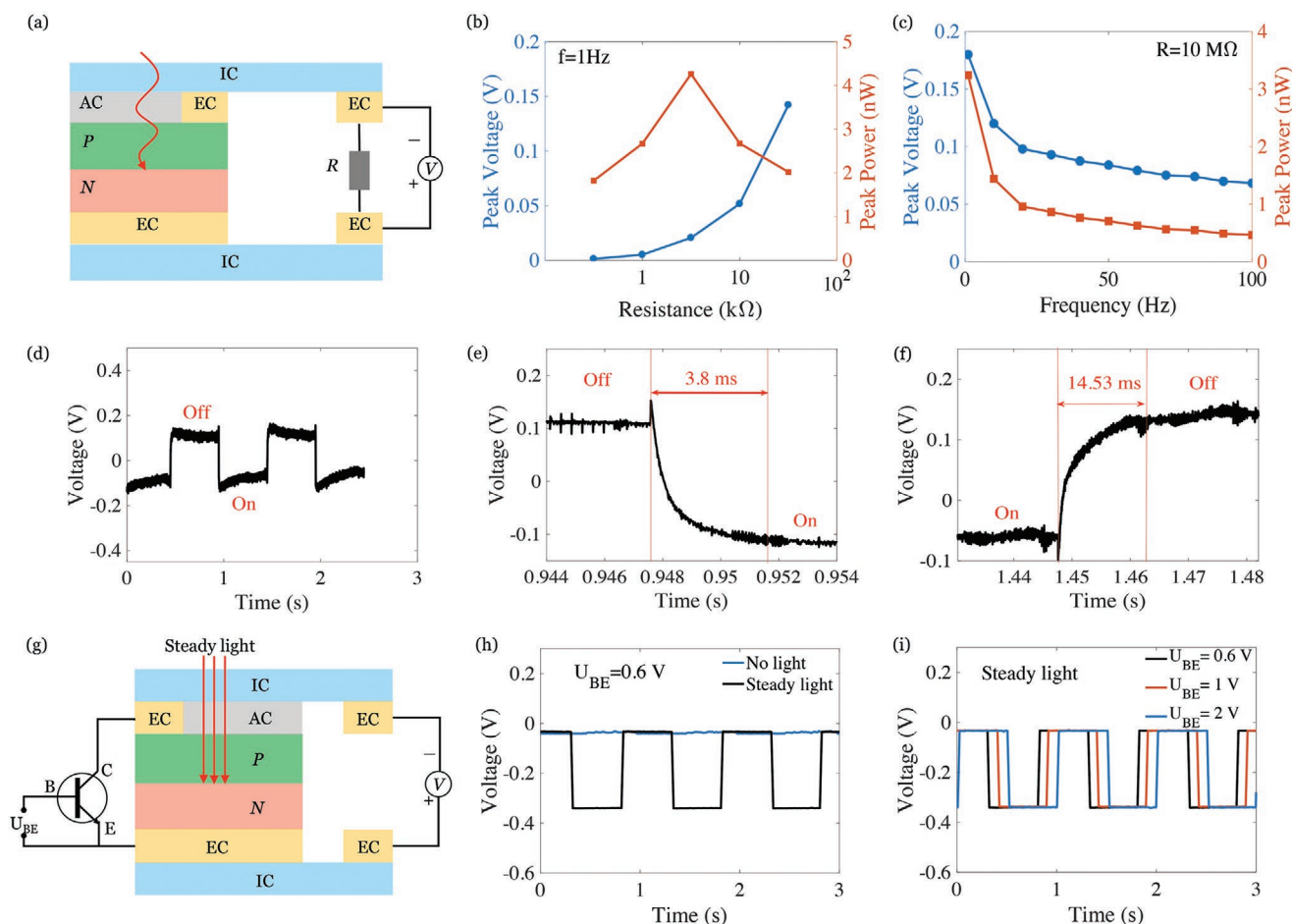


Figure 2. Characteristics of an optoionic sensor. a) A semiconductor photodiode is connected to two ionic conductors (ICs). The top IC contacts both an electronic conductor (EC) and an antireflection coating (AC) of the photodiode. The bottom IC contacts with an EC of the photodiode. The two ICs connect to a voltmeter and a resistor R . b) For several values of R , when a light is switched on and off at a frequency of 1 Hz, the voltmeter records the voltage. Plotted are the peak voltage and peak power. c) The peak voltage and peak power at various on-and-off frequencies of light and with a fixed resistor of $R = 10 \text{ M}\Omega$. In (b) and (c), the sample set for each data point is $n > 20$ cycles, the deviation between cycles is too small to add error bars. d) The open-circuit voltage is measured when the light is switched on and off. e) The transition time of voltage when the light is switched on. f) The transition time of voltage when the light is switched off. g) Shine a steady light on the photodiode, switch on and off a transistor connected to the photodiode by applying U_{BE} , and measure the voltage between the two ionic conductors. h) When the transistor is switched on and off, the voltage between the two ionic conductors is zero when the light is off and is cyclic when the light is steady. Square signal applied to the transistor: $U_{BE} = 0.6 \text{ V}$, $f_T = 1 \text{ Hz}$, and duty cycle = 50%. i) The voltage between the ionic conductors when the transistor is switched on and off at several values of U_{BE} .

3. Photosensitive Skin

3.1. Stiff Electronic Islands and Soft Ionic Bridge

Given the characterization of the single optoionic sensor, we next develop a photosensitive skin with multiple sensors (Figure 3). Three photodiodes are attached to a dielectric layer (Figure 3a), and each is connected to a multi-channel voltmeter through ionic cables in the configuration of Figure S2e, Supporting Information. When a beam of white light focuses on the photodiode in the middle, open-circuit voltages of three ionic cables are recorded simultaneously. The amplitude of the voltage is related to the local intensity of irradiation. We also study other arrangements using a common ground or a matrix (Figure S10, Supporting Information). In general, a photosensitive skin takes the form of islands and bridges. The photodiodes

(the islands) convert light to electrical signals, and the hydrogels (the bridges) function as stretchable and transparent interconnects (Figure S11, Supporting Information).

3.2. Characteristic Length for Signal Decay

To transmit a signal over a long ionic cable, we recall the transmission behavior of ionic signals. The signal decays negligibly when the length of the ionic cable l is small compared to a characteristic length $\sqrt{bd/\omega\rho\epsilon}$, where b is the thickness of the ionic conductor, d is the thickness of the dielectric, ω is the frequency of the signal, ρ is the resistivity of ionic conductor, ϵ is the permittivity of dielectric.^[9] Taking representative values, $b = 3 \text{ mm}$, $d = 0.5 \text{ mm}$, $\omega = 100 \text{ Hz}$, $\rho = 200 \text{ }\Omega\text{m}$ (for hydrogels without salts), and $\epsilon = 10^{-11} \text{ F m}^{-1}$, we find that the characteristic length

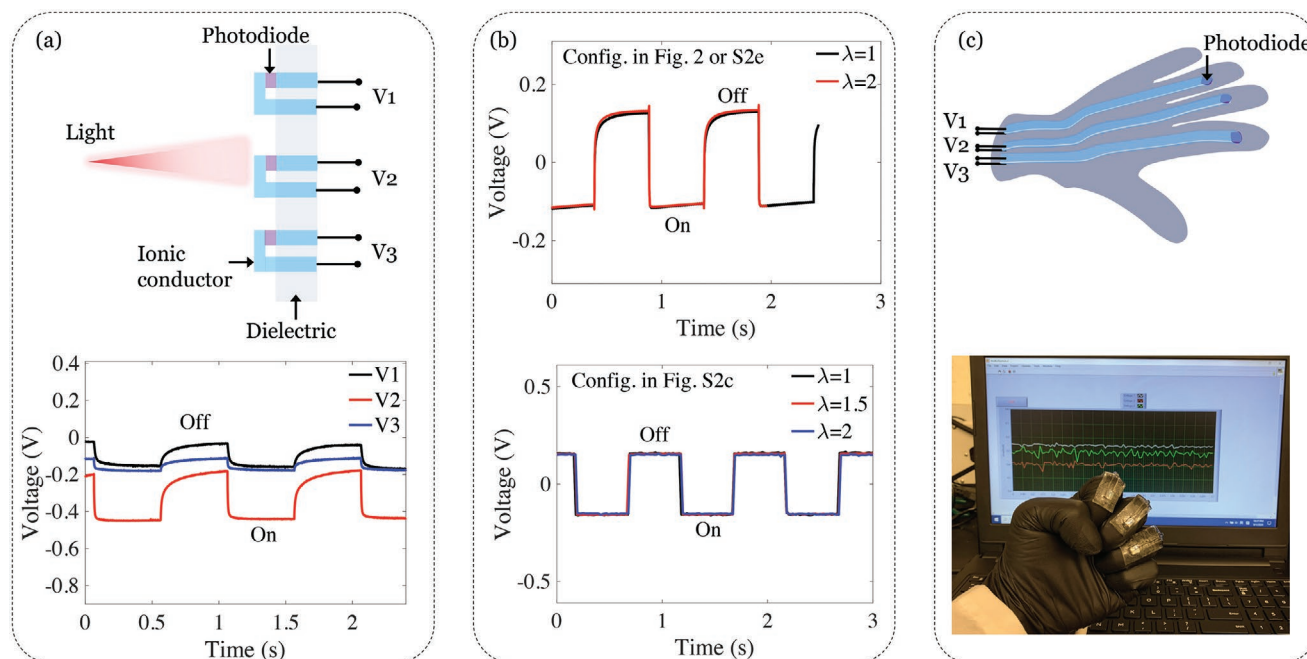


Figure 3. Photosensitive skin. a) When a beam of light shines on a three-channel photosensitive skin, the voltages of the three channels are different. b) The photosensitivity is independent of the stretch. c) When optoionic sensors are attached to a glove, the movements of the hand generate signals.

is $\sqrt{bd/\omega\mu\epsilon} = 2.7$ m. The length of the cable in this work is 4.5 cm, which is much shorter than the characteristic length.

3.3. Stretch-Independent Sensing

The electrical signals are measured at the ends of the ionic cables away from the photodiodes. It is also desirable that the measured electrical signals depend on the locations of the photodiodes, but not on the stretches of the ionic cables. To ascertain the independence of the open-circuit voltage on stretch, we place a photodiode in the chamber and pull the ionic cable to different stretches. The measured open-circuit voltages at different stretches are the same (Figure 3b; Figure S12 and Video S1, Supporting Information).

3.4. Spatial Sensing of Environmental Lights

To demonstrate the interactions between the photosensitive skin and environmental lights, we attach the photosensitive skin on a glove and record the signals while the gloved hand is moving (Figure 3c and Video S2, Supporting Information). Since the deformation of bending fingers has a negligible effect on the signal, the temporospatial variation of the signal is due to the orientation of photodiodes and the intensity of the light source. In Video S2, Supporting Information, the sensors on the glove are exposed to multiple light sources. Before and after the glove moves under the LED lights inside the chamber, the signals monitored on the screen are voltages generated by the environmental light. The fluctuations of the curves are the noise. We calculate the minimum signal-to-noise ratio is three at the first second of the video. As we have shown before (Figure 3a and

Figure S10, Supporting Information), the fluctuation in voltage (i.e., the noise) is much smaller when the sensor is placed on a plastic plate in the chamber. The large fluctuations observed for the sensors on the glove are likely due to small and random movements of the hand. Potential applications of photosensitive skins include stretchable cameras, complex eyes, and rollable light writable screens (Figure S11, Supporting Information).

4. Light-Triggered Neuromuscular Response

4.1. Functional Mimicry of Ionic Processes

Our next experiment is inspired by light-triggered neuromuscular responses, such as a blink of the eye in response to light (Figure 4a).^[15–17] The light excites an ionic signal (action potential) in neurons on the sensing organ. The ionic signal travels along the axon, passes the neuromuscular junction between the neuron and the muscle cell,^[18] and excites muscle cells. The action potential on muscle cells travels to myofibrils and causes the deformation of muscle. Both the signal transmission across neuromuscular junctions by releasing neurotransmitters and the deformation of muscles involve the biochemical reaction that consumes energy stored in ATPs. In our analogy, we employ an ionic cable to mimic the axon, a transistor to mimic the neuromuscular junction, an electrochemical reaction to mimic the biochemical reaction, the deformation of the polyelectrolyte to mimic the deformation of muscles, and a battery to mimic the energy source (Figure 4b). The ionic signal generated by the optoionic sensing is used to control the voltage between the base (B) and the collector (C) of the transistor. The transistor, battery, electrodes, and polyelectrolyte consist of a circuit. We use three photodiodes in series to achieve the voltage threshold

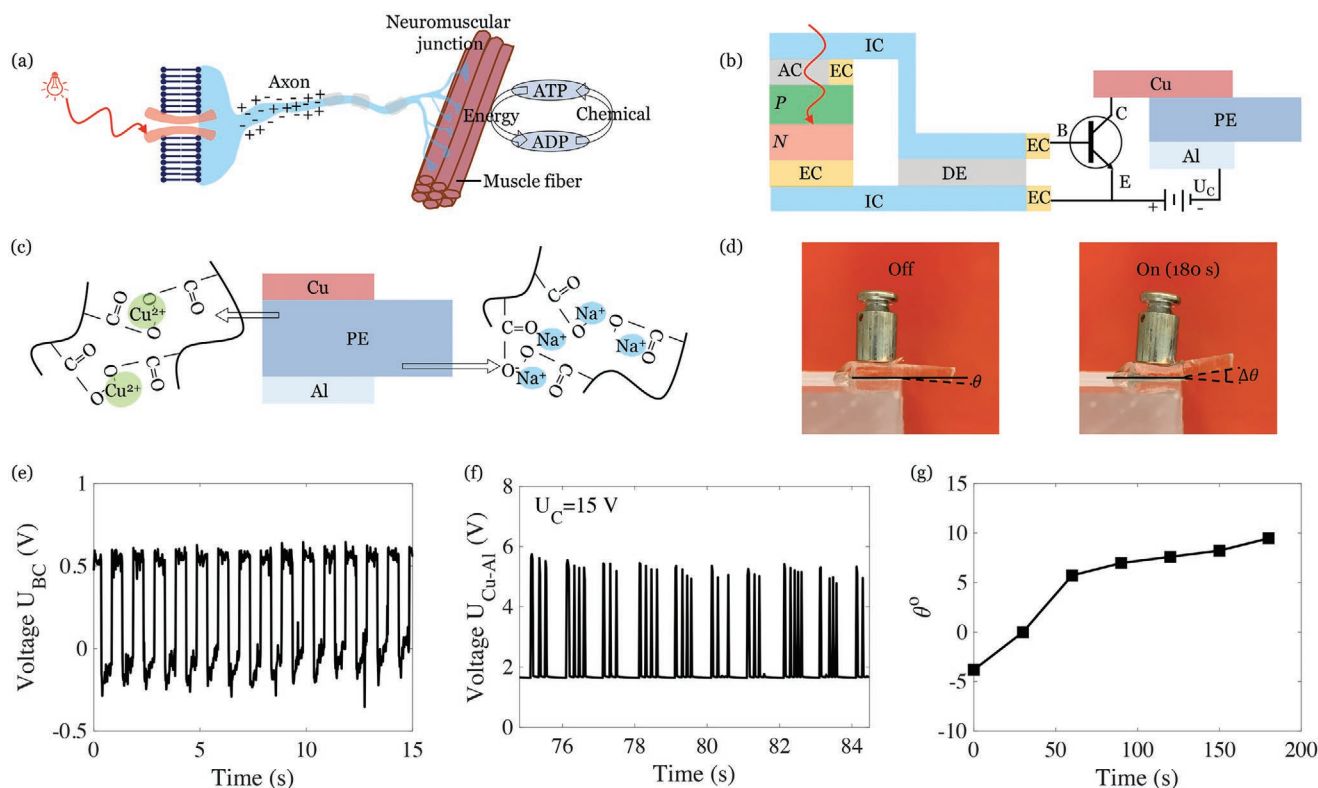


Figure 4. Mimicking a photosensitive neuromuscular response. a) For the eye, a light generates an electrical signal at a photoreceptor cell. The electrical signal travels through an axon, passes neuromuscular junctions, and triggers a muscle to contract. The contraction draws energy from ADP-ATP cycles. b) For an optoionic sensor, a light generates electron-hole pairs in a photodiode, charges the two photodiode/hydrogel interfaces, and induces a voltage. This voltage transmits through an ionic cable, turns on a transistor, and triggers copper to electrolyze. The electrolysis draws energy from a battery. Copper ions coacervate polyelectrolyte chains and bend the beam. DE: dielectric elastomer. PE: polyelectrolyte. E: emitter of the transistor. B: base of the transistor. C: collector of the transistor. Cu: copper. Al: aluminum. c) A sodium polyacrylate is sandwiched between copper and aluminum. When copper electrolyzes, polyelectrolyte chains coacervate near copper, but not aluminum. This asymmetry bends the polyelectrolyte beam. d) The bending angle of the polyacrylate hydrogel. e) The voltage generated between the base and the collector in response to light turned on-and-off at a frequency of 1 Hz. f) The voltage between copper and aluminum. g) The bending angle increases in time.

that switches the transistor on. When electrons flow from the copper electrode to the anode of the battery, an electrochemical reaction occurs in the copper/polyelectrolyte/aluminum electrochemical cell.^[19] The copper ions get into the sodium polyacrylate and increase the crosslink density.^[19] Polyacrylate chains coacervate near copper, but not aluminum (Figure 4c). The asymmetry in the crosslink density across the thickness of polyelectrolyte causes water to migrate, which bends the beam (Figure 4d and Video S3, Supporting Information).

4.2. Light-Triggered Actuation

The voltage U_{BC} between the base and the collector and the voltage U_{EC} between the collector and the emitter are measured under the condition of 1 Hz irradiation of white light (Figure 4e,f). The electrochemical reaction voltage shows a 3–5-folds sub-frequency. This may be due to the fact that we use three photodiodes in series to achieve the voltage threshold U_{BC} of the transistor, and these photodiodes interact separately with the transistor. We characterize the bending of the polyelectrolyte cantilever beam by the angle between the bottom plane of

the beam and the horizontal reference (Figure 4g). A 10° angle is achieved in 1 min, and a 15° angle in 3 min. Although such animation is slow, the ionic signals prevail in stimulation, conduction, reaction, and deformation. Compared to the biological process, the unit size in biology is very small, which fastens the ionic processes ($\text{time} \approx \text{length}^2/\text{diffusivity}$), and the number of units is enormous, which amplifies the amplitude and speed of the actuation. Due to the specific electrochemical reaction, the bending actuation is not reversible by changing the voltage polarization. However, reversible electrochemical reactions and ionic polymer-metal composite actuators can be designed to achieve reversible electric actuators.^[20]

4.3. Opportunities for Neuron Activation

To connect the optoionic transduction to artificial nerves, the choice of ionic conductors can be consistent with the requirements of depolarization or hyperpolarization of nerve signals. The transmembrane potential of neurons is ≈ 70 mV. The large family of ionic conductors provides a rich selection pool for the required scenarios. We replace the polyacrylamide hydrogel

with three kinds of ionic conductors: polycation hydrogel, polyanion hydrogel, and ionogel.^[21,22] In the same configuration, different ionic conductors show distinct base voltages, voltage changes, and profiles (Figure S13, Supporting Information). Other ionic conductors, such as poly-zwitterions^[23] and ionoelastomers,^[24] are also applicable.

In summary, we study the physics of optoionic transduction in photodiode-hydrogel hybrids. We use these hybrids to mimic biological functions in optoionic transduction, photosensitive skin, and light-triggered actuation. Potential applications of optoionic sensing include wearable and implantable devices, as well as soft robots.

5. Experimental Section

Polyacrylamide Hydrogel: The monomer (Acrylamide, AAm), the salt (lithium chloride, LiCl), the crosslinking agent (N,N'-methylenebisacrylamide, MBAA), the photoinitiator (2-Hydroxy-4'-(2-hydroxyethoxy)-2-methylpropiophenone, I-2959), and ethyl alcohol were purchased from Sigma Aldrich Co. The monomer was dissolved in deionized water with a concentration of 2 M. The crosslinker was dissolved in deionized water with a concentration of 0.1 M. The photoinitiator was dissolved in ethyl alcohol with a concentration of 0.033 g mL⁻¹. Mix the solution of AAm, MBAA, and I-2959 by a ratio of 1 mL: 6.6 μ L: 1.5 μ L. The uniform solution was transferred into an acrylic mold and then cured under a UV lamp (power: 50 W, wavelength: 365 nm) for 2 h. For polyacrylamide hydrogels with salts, the concentration of lithium chloride was 0.1 M.

Ionogel: 1-ethyl-3-methylimidazolium ethylsulfate ([C₂mim][EtSO₄], ionic liquid), acrylic acid (AA, monomer), Poly(ethylene glycol) diacrylate (crosslinker), and α -ketoglutaric acid (initiator) were purchased from Sigma Aldrich Co. Dissolve the monomer into the ionic liquid at 1 mol L⁻¹. Add the cross-linker and the initiator at 0.6 mol and 1 mol% of the monomer, respectively. After the mixture, transfer the solution into molds made of acrylic. Then put the molds under a UV lamp (power: 50 W, wavelength: 365 nm) for 2 h.

Polyelectrolyte: (1) Polyanion hydrogel monomer: 3-sulfopropyl acrylate potassium (SAPS, Sigma Aldrich). (2) Polycation hydrogel monomer: (3-acrylamidopropyl) trimethyl ammonium chloride (APTAC, Sigma Aldrich). To make both polyelectrolyte hydrogels, the monomer concentration was 2 M. For each 10 mL monomer aqueous solution, add 300 μ L MBAA solution and 200 μ L I-2959 solution with both concentrations of 0.1 M. The solution was transferred in acrylic molds and placed under a UV lamp for 2 h.

Sodium Polyacrylate Hydrogel: The monomer (sodium acrylate, Sigma Aldrich) was dissolved in distilled water at a concentration of 5 M with the mole ratio of crosslinker MBAA to monomer 1:200.^[19] In a 10 mL monomer-crosslinker solution, 200 μ L I-2959 ethanol solution (0.1 M) was added. The mixed solution was transferred in acrylic molds and placed under a UV lamp for 2 h. After polymerization, the hydrogel was placed in a tank of distilled water for 1 day.^[19] After the full swelling, a strip of poly(sodium acrylate) gel was cut with the dimensions of 42 mm \times 10 mm \times 4.5 mm.

Acrylic Mold: The acrylic molds were cut by a laser cutter (Helix, 75W). For molds to make ionic conductors, the removed acrylic was in the shape of gels, as shown in Figure 1C. The shape has two parts. One has the dimensions of 40 mm \times 3 mm \times 3 mm, and the other has the dimensions of 15 mm \times 15 mm \times 3 mm. For molds to make sodium polyacrylate hydrogel, the size of the mold was 50 mm \times 10 mm \times 1.5 mm.

Electronic Devices: The solderable planar photodiode was SLCD-61N2 (sensing wavelength from 400 to 1100 nm and optimized at 900 nm). The photodiode is characterized in Figure S14, Supporting Information. The equivalent resistance and the junction capacitance of the photodiode were measured using Hewlett Packard 34401A multimeter and BK Precision Models 830C/890C capacitance meter. The *p*-type wafer (ID:2723, P/B, <100>, resistivity 0.001–0.005 Ω cm) was from University

Wafer. The bipolar transistor was a C1815 silicon *n*pn transistor. The electrode deposited on photodiodes was gold. The electronic conductors that connect ionic conductors to the measurement kit were aluminum foils, except the graphite paper in Figure S8, Supporting Information. Tin was sold on gold electrodes in the direct measurements of photodiodes. The interconnectors in circuits were insulated copper wires (0.5 mm). The measurement kit for voltage was NI USB-6210. The light source in the chamber was a 10 W LED cool white SMD chip (9–12 V) bought from Amazon. Unless otherwise specified, the voltage applied to LED was $U_{LED} = 8$ V. The irradiation frequency of light was controlled by NI USB-6002. The U_{BE} applied to the transistor in the measurement of Figure S9, Supporting Information was through a function generator Keysight 33500B, and others were through NI USB-6002. The direct voltage/current source was Hewlett Packard (E3610A) DC power supply. All control and data acquisition programs were in LabView 2017 on a Dell laptop. Data were processed in Matlab. The transient simulations of equivalent circuits in Figure S3, Supporting Information were done in CircuitLab, where the step time of simulation was 10 μ s.

Assembly of Optoionic Sensors: As illustrated in Figure 1c, each layer of the ionic conductor was insulated by a dielectric elastomer VHB4905 (3M). The ionic conductors were directly attached to both sides of photodiodes. The chemical bonding between polymers and silicones was recommended but not necessary in experiments. In some configurations in Figure S2, Supporting Information, the gold electrodes on commercial photodiodes were removed by the scratch of the blade. Detailed assemblies of configurations in Figure S2, Supporting Information are described in supplementary context 1.1.

Measurement Chamber: An acrylic chamber has dimensions of 9.5 cm \times 11.5 cm \times 17.5 cm. The LED light was installed in the center of the top wall, and the sample was fixed in the center of the bottom wall. The outside of the chamber was covered with aluminum foils.

SEM Imaging: The imaging was done through an ultra plus field emission scanning electron microscope (Zeiss) using a 3 keV energy electron beam.

Supporting Information

Supporting Information is available from the Wiley Online Library or from the author.

Acknowledgements

This work was supported by NSF Materials Research Science and Engineering Centers (Grant DMR-2011754). B.C. thanks Dr. Quan Jiao at Harvard University for the help of SEM imaging.

Conflict of Interest

The authors declare no conflict of interest.

Data Availability Statement

Research data are not shared.

Keywords

ionic conductors, neuromuscular junctions, photodiodes, photoreceptors, stretchable sensors

Received: July 4, 2021
Revised: September 21, 2021
Published online:

- [1] L. Luo, *Principles of Neurobiology*, 2nd ed., Garland Science, Boca Raton, FL **2020**, p. 760.
- [2] P. Cheng, X. Tian, W. Tang, J. Cheng, J. Bao, H. Wang, S. Zheng, Y. Wang, X. Wei, T. Chen, H. Feng, T. Xue, K. Goda, H. He, *Cell Res.* **2021**, 37, 758.
- [3] V. R. Schild, M. J. Booth, S. J. Box, S. N. Olof, K. R. Mahendran, H. Bayley, *Sci. Rep.* **2017**, 7, 46585.
- [4] J. Saroia, W. Yanen, Q. Wei, K. Zhang, T. Lu, B. Zhang, *Bio-Des. Manuf.* **2018**, 1, 265.
- [5] C. Wan, P. Cai, X. Guo, M. Wang, N. Matsuhisa, L. Yang, Z. Lv, Y. Luo, X. J. Loh, X. Chen, *Nat. Commun.* **2020**, 11, 4602.
- [6] F. Jabr, Blindsight: Animals That See without Eyes, <https://www.scientificamerican.com/article/seeing-without-eyes/> (accessed: August 2012).
- [7] J. B. Bryson, C. B. Machado, M. Crossley, D. Stevenson, V. Bros-Facer, J. Burrone, L. Greensmith, I. Lieberam, *Science* **2014**, 344, 94.
- [8] B. Chen, Y. Bai, F. Xiang, J.-Y. Sun, Y. M. Chen, H. Wang, J. Zhou, Z. Suo, *J. Polym. Sci., Part B: Polym. Phys.* **2014**, 52, 1055.
- [9] C. H. Yang, B. Chen, J. J. Lu, J. H. Yang, J. Zhou, Y. M. Chen, Z. Suo, *Extreme Mech. Lett.* **2015**, 3, 59.
- [10] B. Chen, W. Sun, J. Lu, J. Yang, Y. Chen, J. Zhou, Z. Suo, *J. Appl. Mech.* **2020**, 88, 031016.
- [11] H. Sheng, X. Wang, N. Kong, W. Xi, H. Yang, X. Wu, K. Wu, C. Li, J. Hu, J. Tang, J. Zhou, S. Duan, H. Wang, Z. Suo, *Extreme Mech. Lett.* **2019**, 30, 100510.
- [12] S. Park, H. Yuk, R. Zhao, Y. S. Yim, E. W. Woldegebriel, J. Kang, A. Canales, Y. Fink, G. B. Choi, X. Zhao, P. Anikeeva, *Nat. Commun.* **2021**, 12, 3435.
- [13] C. Keplinger, J.-Y. Sun, C. C. Foo, P. Rothmund, G. M. Whitesides, Z. Suo, *Science* **2013**, 341, 984.
- [14] Medical Physics, <https://www3.nd.edu/~nsl/Lectures/mphysics/> (accessed: April 2004).
- [15] E. M. Ullrich-Luter, S. Dupont, E. Arboleda, H. Hausen, M. I. Arnone, *Proc. Natl. Acad. Sci. U. S. A.* **2011**, 108, 8367.
- [16] D. C. Plachetzki, C. R. Fong, T. H. Oakley, *BMC Biol.* **2012**, 10, 17.
- [17] Y. Xiang, Q. Yuan, N. Vogt, L. L. Looger, L. Y. Jan, Y. N. Jan, *Nature* **2010**, 468, 921.
- [18] M. Gonzalez-Freire, R. de Cabo, S. A. Studenski, L. Ferrucci, *Front. Aging Neurosci.* **2014**, 6, 208.
- [19] E. Palleau, D. Morales, M. D. Dickey, O. D. Velez, *Nat. Commun.* **2013**, 4, 2257.
- [20] B. Bhandari, G.-Y. Lee, S.-H. Ahn, *Int. J. Precis. Eng. Manuf.* **2012**, 13, 141.
- [21] S. Werner, M. Haumann, P. Wasserscheid, *Annu. Rev. Chem. Biomol. Eng.* **2010**, 1, 203.
- [22] B. Chen, J. J. Lu, C. H. Yang, J. H. Yang, J. Zhou, Y. M. Chen, Z. Suo, *ACS Appl. Mater. Interfaces* **2014**, 6, 7840.
- [23] S. Paschke, K. Lienkamp, *ACS Appl. Polym. Mater.* **2020**, 2, 129.
- [24] H. J. Kim, B. Chen, Z. Suo, R. C. Hayward, *Science* **2020**, 367, 773.